DOI: https://doi.org/10.14311/TPFM.2025.008

ON THE SIGNIFICANCE OF FLOW VORTICITY FOR HEMOLYSIS MODELING

N. Dirkes, M. Behr

Chair for Computational Analysis of Technical Systems, RWTH Aachen University, Schinkelstr. 2, 52062 Aachen, Germany

Abstract

Flow-induced red blood cell damage (*hemolysis*) occurs through excessive deformation of red blood cells. Simple hemolysis models are based on fluid stress, but typically neglect the antisymmetric part of the velocity gradient tensor, i.e., *flow vorticity*. We show that this is not always an admissible simplification, as vorticity affects cell orientation and deformation. We introduce a systematic theory for the influence of vorticity on hemolysis. This theory helps explain differences observed experimentally between shear flow and extensional flow. We suggest an alternative definition of the scalar representative stress that incorporates vorticity effects into stress-based hemolysis models.

Keywords: hemodynamics, hemolysis, red blood cell.

1 Introduction

Red blood cell damage (*hemolysis*) occurs when flow forces induce excessive deformation or rupture of red blood cells (RBCs). While physiological flow conditions are generally well tolerated by RBCs, blood-handling medical devices can expose them to high stresses. Hemolysis is therefore a key factor in the design process of blood-handling medical devices. The numerical prediction of this phenomenon is based on computational fluid dynamics (CFD) simulations. Simple *stress-based* hemolysis models post-process the CFD results by reducing three-dimensional fluid stresses to representative scalar stresses. *Flow vorticity*, i.e., the antisymmetric part of the velocity gradient, is generally neglected in these models (comp. [1, 2]). More complex *strain-based* models resolve RBC deformation and orientation. This way, they can account for the viscoelastic behavior of the RBC membrane and take into account all flow components, including vorticity.

Stress-based models are computationally efficient, but have historically shown large deviations from experimental data [3]. At the same time, there have been discussions on the significance of extensional stresses over shear stresses for hemolysis [4–6]. In this work, we attempt to reconcile these observations by systematically comparing stress-based and strain-based hemolysis models. This will allow us to quantify the influence of vorticity on model predictions and provide insights into the role of extensional stresses in hemolysis.

This paper is structured as follows: In Section 2, we provide a brief overview of hemolysis modeling and the role of vorticity. We define quantitative measures to describe the influence of vorticity. In Section 3, we present a selection of test cases to illustrate the effect of vorticity on hemolysis. In Section 4, we discuss how our findings help explain experimental observations on the significance of extensional stresses over shear stresses for hemolysis. In Section 5, we summarize our results.

2 Background

Flow-induced hemolysis occurs when the membrane of an RBC ruptures or forms pores. The hemoglobin that is normally confined within the cell is then released into the surrounding blood plasma. This process is described by the index of hemolysis IH, which quantifies the amount of hemoglobin released into the plasma relative to the total hemoglobin content of the blood. The most popular models for hemolysis are power-law models that correlate fluid stress τ and exposure time t to the index of hemolysis IH:

$$IH = C\tau^{\alpha}t^{\beta}\,, \tag{1}$$

where α, β, and C are empirical parameters. Experiments to determine these parameters are typically conducted by exposing blood to a range of shear stresses and exposure times in a rheometer. The amount of released hemoglobin is then measured in-vitro. The fluid stress τ reduces the three-dimensional stress tensor to a representative scalar. This reduction corresponds essentially to defining a norm $||\cdot||$. For Newtonian fluids in particular, we can express this relation as a norm on the rate of strain tensor $\mathbf{E}$:

$$\tau = 2\mu||\mathbf{E}||\,, \qquad \mathbf{E} = \frac{1}{2}\Big(\big(\boldsymbol{\nabla}\mathbf{u}\big) + \big(\boldsymbol{\nabla}\mathbf{u}\big)^{\mathbf{T}}\Big)\,. \tag{2}$$

Popular choices for the norm are provided by Bludszuweit [1] and Faghih and Sharp [6]:

$$||\mathbf{E}||_{\mathrm{B}} = \frac{1}{\sqrt{3}}\sqrt{E_{xx}^2 + E_{yy}^2 + E_{zz}^2 - (E_{xx}E_{yy} + E_{yy}E_{zz} + E_{zz}E_{xx}) + 3(E_{xy}^2 + E_{xz}^2 + E_{yz}^2)}\,, \tag{3a}$$

$$||\mathbf{E}||_{\mathrm{FS}} = \frac{1}{\sqrt{3}}\sqrt{1142\big[E_{xx}^2 + E_{yy}^2 + E_{zz}^2 - (E_{xx}E_{yy} + E_{yy}E_{zz} + E_{zz}E_{xx})\big] + 3(E_{xy}^2 + E_{xz}^2 + E_{yz}^2)}\,. \tag{3b}$$

The main feature of the Faghih-Sharp (FS) norm (3b) compared to the Bludszuweit norm (3a) is the stronger emphasis on the diagonal components of the strain tensor. This is motivated by experimental observations indicating that red blood cells are more sensitive to extensional stresses than to shear stresses [6]. Models given by Eqs. (1) to (3) are subsequently referred to as *stress-based* hemolysis models, since they are based on the instantaneous fluid stress. We will define the subscript of the representative scalar stress according to the choice of the norm, i.e., $\tau_{\mathrm{B}} = 2\mu||\mathbf{E}||_{\mathrm{B}}$ and $\tau_{\mathrm{FS}} = 2\mu||\mathbf{E}||_{\mathrm{FS}}$, respectively.

Notably, any models of this form do not take into account the antisymmetric part of the velocity gradient, i.e., the vorticity $\mathbf{W} = \frac{1}{2}\Big(\big(\boldsymbol{\nabla}\mathbf{u}\big) - \big(\boldsymbol{\nabla}\mathbf{u}\big)^{\mathbf{T}}\Big)$. In order to investigate the influence of vorticity, we employ a more complex hemolysis model that explicitly resolves red blood cell deformation and orientation, the tank-treading morphology model (TTM) [7]. In this work, we restrict ourselves to the Lagrangian formulation of the model, i.e., the application along particle trajectories through the flow field. The model describes red blood cells as three-dimensional ellipsoids with semi-axes $\boldsymbol{\Lambda} = (\lambda_1, \lambda_2, \lambda_3)$ and orientation $\mathbf{Q}$. It describes the evolution of these cells along their trajectories through the flow field by a system of differential and algebraic equations:

$$\frac{\mathrm{d}\lambda_i}{\mathrm{d}t} = -f_1\left(\lambda_i - \frac{3\lambda_1\lambda_2\lambda_3}{\lambda_1\lambda_2 + \lambda_2\lambda_3 + \lambda_3\lambda_1}\right) + 2f_2\lambda_i\tilde{E}_{ii}\,, \tag{4a}$$

$$\tilde{\mathbf{E}} = \mathbf{Q}^{\mathbf{T}}\mathbf{E}\mathbf{Q}\,, \qquad \mathbf{Q} = \begin{cases} \mathbf{Q}_\star(\boldsymbol{\Lambda}, \mathbf{E}, \mathbf{W}), & \text{tank-treading}\,, \\ \mathbf{0}, & \text{tumbling}\,. \end{cases} \tag{4b}$$

Here, Eq. (4a) describes the evolution of the deformation, while Eq. (4b) describes the orientation of the cell. Due to its derivation, the Lagrangian formulation of the model corresponds essentially to a more computationally efficient version of the well-established Arora model [8]. For more details, we refer to Dirkes et al. [7]. An open-source implementation of the model is available (`https://github.com/nicodirkes/HemTracer`). Based on the cell deformation $\boldsymbol{\Lambda}$ predicted by the model, we compute a so-called effective scalar stress

$$\tau_{\mathrm{eff}} = \mu G_{\mathrm{eff}}(\boldsymbol{\Lambda})\,, \tag{5}$$

as a measure of tension in the cell membrane. Through the model equations (4), this quantity takes into account both $\mathbf{E}$ and $\mathbf{W}$ and can be used in the power-law correlation (1) as alternative to the fluid stress (2). Models given by the form Eqs. (1), (4) and (5) are referred to as *strain-based* hemolysis models, as they are based on membrane strain.

For the analysis, we will define a dimensionless number ν that weighs the strength of vorticity against the strength of strain:

$$\nu = \frac{||\mathbf{E}||_{\mathrm{B}} - ||\mathbf{W}||_{\mathrm{B}}}{||\mathbf{E}||_{\mathrm{B}} + ||\mathbf{W}||_{\mathrm{B}}}\,. \tag{6}$$

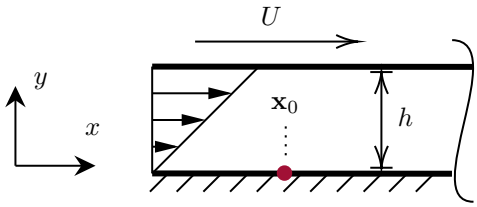

(a) Configuration

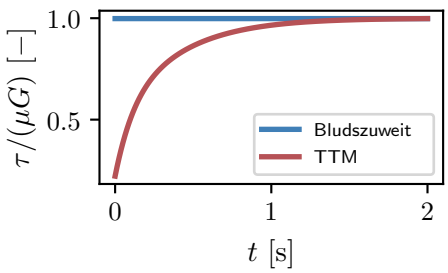

(b) Effective and instantaneous stress at $\mathbf{x}_0$ over time

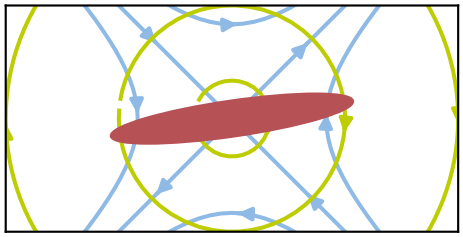

(c) Final cell shape and orientation at $\mathbf{x}_0$

Figure 1: Plane Couette flow

For $\nu > 0$, the flow is dominated by strain, with a purely extensional flow for $\nu = 1$. Analogously, $\nu < 0$ means that vorticity dominates, with a purely rotational flow for $\nu = -1$. We will show that hemolysis models based on Eqs. (1) and (2) assume $\nu \equiv 0$, which is not always the case in practice. Further, we will show a strong dependence of effective stress (5) on this parameter ν, indicating that vorticity is an important factor in hemolysis modeling, which is not accounted for in simple power-law models. For this purpose, we define a dimensionless deviation between the effective stress and the fluid stress:

$$\delta(\nu) = \frac{\tau_{\text{eff}}(\nu) - \tau_{\text{B}}}{\tau_{\text{B}}} \,. \tag{7}$$

3 Numerical results

To illustrate the methodology, we first present results for a plane Couette flow, as shown in Fig. 1a. Given a shear rate $G = U/h$, we can determine the velocity gradient components as

$$\mathbf{E} = \begin{pmatrix} 0 & G/2 & 0 \\ G/2 & 0 & 0 \\ 0 & 0 & 0 \end{pmatrix}, \quad \mathbf{W} = \begin{pmatrix} 0 & G/2 & 0 \\ -G/2 & 0 & 0 \\ 0 & 0 & 0 \end{pmatrix}, \quad ||\mathbf{E}||_{\text{B}} = ||\mathbf{W}||_{\text{B}} = \frac{G}{2} \,. \tag{8}$$

We thus have $\nu = 0$ for this case. We will now discuss the results for $G = 40{,}000\,\text{s}^{-1}$, but the results for other shear rates are qualitatively similar. For the stress-based model, we observe a constant stress $\tau_{\text{B}} = \mu G$ over time, as shown in Fig. 1b. This is because the flow is steady, so the instantaneous fluid stress is constant in time. For the strain-based model, the effective strain increases over time. This is a characteristic feature of such models, which take into account the viscoelastic properties of the red blood cell membrane. Mathematically, this is reflected in the equation structure of the model, namely a differential dependence of the cell deformation on fluid stress [7]. Conversely, stress-based models following Eq. (2) exhibit a purely algebraic dependence on fluid stress, corresponding to elastic cell response and neglecting any stress history. For this reason, stress-based models can never approximate the temporal delay observed in the strain-based model. Nevertheless, we find that the two models agree in their steady state prediction, i.e., $\tau_{\text{B}} = \tau_{\text{eff}} = \mu G\,,\ t \to \infty$. Consequently, we can say that $\delta(0) = 0$ asymptotically.

Finally, Fig. 1c shows the cell orientation at steady state $t = 2\,\text{s}$, as predicted by the strain-based model. The streamlines in the background indicate the components of the strain tensor $\mathbf{E}$ (blue)

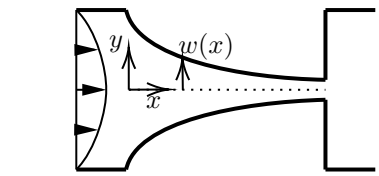

(a) Reference configuration

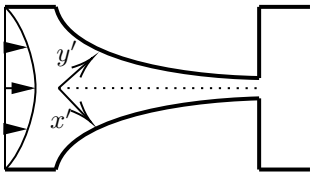

(b) Rotated coordinate system

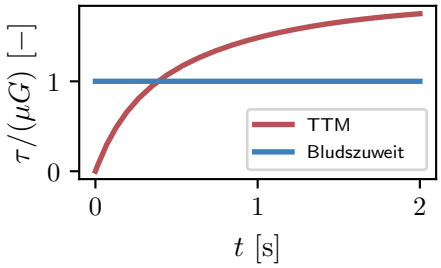

(c) Effective and instantaneous stress

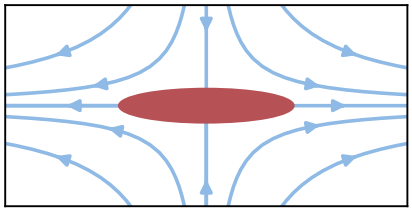

(d) Cell shape and orientation at $t = 2\,\mathrm{s}$

Figure 2: Flow through a hyperbolic contraction.

and the vorticity tensor $\mathbf{W}$ (green). While the strain components attempt to align the cell with the principal direction of tensile strain (bottom left to top right), the vorticity components act to rotate the cell. The resulting orientation represents an equilibrium between these moments.

Next, we investigate the flow through a hyperbolic contraction, as sketched in Fig. 2a. The channel width follows $w(x) \sim 1/x$. Along the centerline, this induces a constant acceleration $u(x) = \epsilon x$. If we set the flow intensity to $\epsilon = G/2$, the velocity gradient takes the form $\boldsymbol{\nabla}\mathbf{u} = \mathbf{diag}(G/2, -G/2, 0)$. The resulting strain and vorticity tensors are given by

$$\mathbf{E} = \begin{pmatrix} G/2 & 0 & 0 \\ 0 & -G/2 & 0 \\ 0 & 0 & 0 \end{pmatrix}, \quad \mathbf{W} = \begin{pmatrix} 0 & 0 & 0 \\ 0 & 0 & 0 \\ 0 & 0 & 0 \end{pmatrix}, \quad ||\mathbf{E}||_{\mathrm{B}} = \frac{G}{2}, \quad ||\mathbf{W}||_{\mathrm{B}} = 0\,. \tag{9}$$

This case thus corresponds to $\nu = 1$. We will discuss results for $G = 20{,}000\,\mathrm{s}^{-1}$, but the results for other intensities are qualitatively similar. As Fig. 2c shows, the stress-based model again predicts a constant representative stress $\tau_{\mathrm{B}} = \mu G$. Since the norm on the strain tensor $\mathbf{E}$ is the same in Eqs. (8) and (9), we obtain the same scalar representative stress as in the plane Couette flow. For the strain-based model, on the other hand, we find a significantly higher effective stress $\tau_{\mathrm{eff}} \approx 2\mu G$ at steady state. In this case, the two models thus do not agree asymptotically and we find $\delta(1) \approx 1$. This indicates that the vorticity has a significant influence on the effective stress, which is not accounted for in the stress-based model.

As Fig. 2d shows, the cell orientation at steady state $t = 2\,\mathrm{s}$ is aligned with the principal direction of strain. This is in contrast to the plane Couette flow, where the cell orientation was in equilibrium between strain and vorticity. The reason for this difference is that there is no vorticity in the hyperbolic contraction ($\nu = 1$), so the cell is not subject to any rotational moments opposing the aligning effect of the strain.

Finally, we note that the FS norm (3b) gives $||\mathbf{E}||_{\mathrm{FS}} \approx 17G \gg ||\mathbf{E}||_{\mathrm{B}}$ for the hyperbolic contraction. This norm thus captures the higher deformation in the hyperbolic contraction compared to the plane Couette flow. However, when defining a coordinate system rotated by 45° (see Fig. 2b), we find

$$\mathbf{E}' = \begin{pmatrix} 0 & G/2 & 0 \\ G/2 & 0 & 0 \\ 0 & 0 & 0 \end{pmatrix}, \qquad ||\mathbf{E}'||_{\mathrm{B}} = ||\mathbf{E}'||_{\mathrm{FS}} = \frac{G}{2}\,.$$

This indicates that the FS norm depends on the coordinate system in which it is applied. The

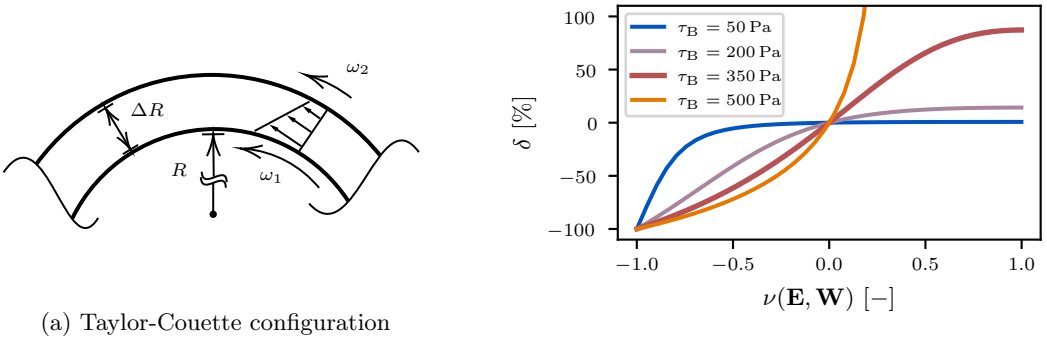

(a) Taylor-Couette configuration

(b) Relative modeling error of stress-based models

Figure 3: Systematic study of the relative modeling error δ of stress-based models across different relative vorticity values ν and fluid stress levels τ_B.

coordinate system defines what is considered a normal stress and what is considered a shear stress. Finding a proper coordinate system is thus crucial for the interpretation of the FS norm.

To investigate the effect of vorticity more systematically, we consider a Taylor-Couette flow with the inner cylinder rotating at an angular velocity ω_1 and the outer cylinder rotating at an angular velocity ω_2. We define the dimensionless gap width $\eta = \frac{R}{R+\Delta R}$ and the dimensionless rotation ratio $\xi = \frac{\omega_2}{\omega_1}$. The Taylor-Couette instability can be avoided if [9]:

$$\xi > \eta^2 \,. \tag{10}$$

In that case, the flow is purely azimuthal, and the velocity components are given by [10]:

$$u_r = u_z = 0\,, \quad u_\theta = Ar + \frac{B}{r}\,, \qquad A = \omega_1 \frac{\xi - \eta^2}{1-\eta^2}\,, \quad B = \omega_1 R^2 \frac{1-\xi}{1-\eta^2}\,.$$

The velocity gradient in cylindrical coordinates is then given by

$$\boldsymbol{\nabla}\mathbf{u} = \begin{pmatrix} \frac{\partial u_r}{\partial r} & \frac{1}{r}\frac{\partial u_r}{\partial \theta} - \frac{u_\theta}{r} & \frac{\partial u_r}{\partial z} \\ \frac{\partial u_\theta}{\partial r} & \frac{1}{r}\frac{\partial u_\theta}{\partial \theta} + \frac{u_r}{r} & \frac{\partial u_\theta}{\partial z} \\ \frac{\partial u_z}{\partial r} & \frac{1}{r}\frac{\partial u_z}{\partial \theta} & \frac{\partial u_z}{\partial z} \end{pmatrix} = \begin{pmatrix} 0 & -A - \frac{B}{r^2} & 0 \\ A - \frac{B}{r^2} & 0 & 0 \\ 0 & 0 & 0 \end{pmatrix}.$$

Decomposing this gradient into strain and vorticity and taking the norm according to Eq. (3a), we obtain at $r = R$:

$$||\mathbf{E}||_B = \omega_1 \frac{1-\xi}{1-\eta^2}\,, \quad ||\mathbf{W}||_B = \omega_1 \frac{\xi - \eta^2}{1-\eta^2}\,, \qquad \nu = \frac{1 - 2\xi + \eta^2}{1-\eta^2}\,,$$

and with some rearranging:

$$\xi = \frac{1}{2}\big(1 + \eta^2 - \nu(1-\eta^2)\big)\,, \qquad \omega_1 = \frac{\tau_B}{2\mu}\frac{1-\eta^2}{1-\xi}\,. \tag{11}$$

This result is important for two reasons. First, it shows that for $\nu < 1$, we have

$$\xi > \frac{1}{2}\big(1 + \eta^2 - 1 \cdot (1-\eta^2)\big) = \eta^2\,,$$

so we guarantee stability of the flow by condition (10). Interestingly, the pure strain case $\nu = 1$ corresponds to the theoretical stability limit $\xi = \eta^2$. Second, Eq. (11) shows that given a gap width η, we can choose rotation rates ω_1 and ω_2 such that we obtain a stable system for any desired value of the vorticity parameter $\nu \in (-1, 1)$ and any stress level τ_B. This allows us to systematically investigate the influence of vorticity at different stress levels.

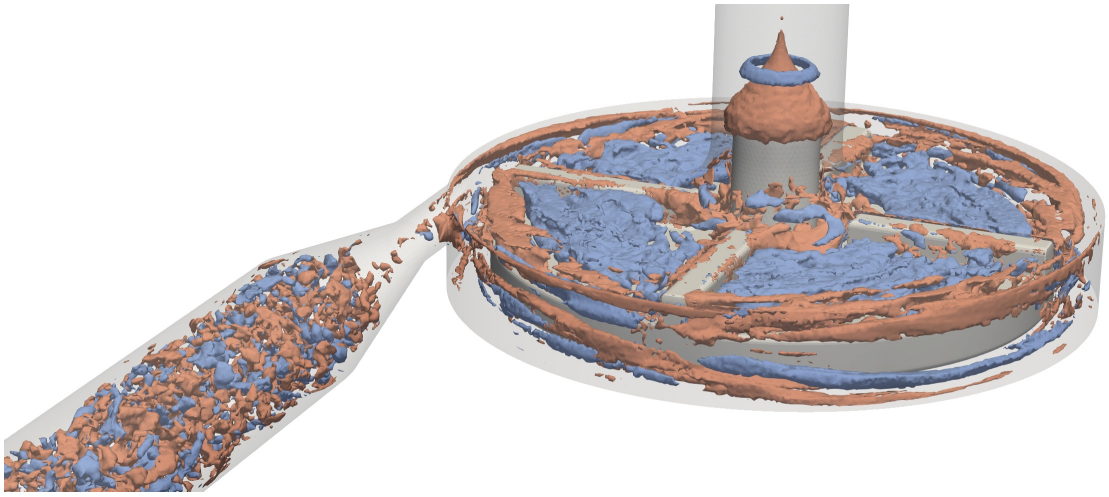

Figure 4: Contours of $\nu = -0.35$ (blue) and $\nu = 0.35$ (red) throughout the FDA benchmark blood pump.

We consequently simulate the Taylor-Couette flow for a gap size $\eta = 0.99$ and a range of vorticity parameters $\nu \in (-1, 1)$ and fluid stresses $\tau_B \in \{50\,\text{Pa}, 200\,\text{Pa}, 350\,\text{Pa}, 500\,\text{Pa}\}$. We compare the steady-state predictions of the stress-based and strain-based models by evaluating the relative error (7). The results are shown in Fig. 3b. For $\nu = 0$, i.e., simple shear, the predictions of the two models agree, as analyzed for the simple Couette flow above. For $\nu \to 1$, the strain-based model predicts a significantly higher effective stress than the stress-based model. This is consistent with the results for the hyperbolic contraction. With increasing levels of fluid stress, the deviation between the two models increases. This indicates that the influence of vorticity on the effective stress becomes more pronounced at higher stress levels. For $\nu \to -1$, the strain-based model predicts essentially no effective stress, as the strong vorticity keeps the cells rotating, preventing them from aligning with the principal direction of strain and evenly distributing the stress. In between these characteristic cases, there is a continuous and monotonic dependence of the deviation on the vorticity parameter, highlighting the systematic influence of vorticity on red blood cell deformation.

Last, we investigate the range of ν that is relevant in practical applications. For this purpose, we analyze the FDA benchmark blood pump. We conduct a CFD simulation at a rotor speed of 3500 rpm and a flow rate of 2.5 L/min. We utilize a multiple reference frame approach to model the rotating impeller at steady state. The flow field is employed to compute the vorticity parameter (6) throughout the pump. The results are shown in Fig. 4. We find extreme values of $\nu = \pm 0.93$ in the pump. The impeller exhibits large connected regions of strain-dominated flow ($\nu = 0.35$) in between the blades. Towards the outer walls, there are large areas of vorticity-dominated flow ($\nu = -0.35$).

4 Discussion

The test cases analyzed in this work are well-established benchmarks for hemolysis modeling. They have been studied extensively both experimentally and numerically. However, there is no unified interpretation of the results, namely the stronger deformation in the hyperbolic contraction compared to the plane Couette flow. Most recently, Faghih and Sharp [6] attempted to reconcile these observations with classical stress-based models by defining an alternative measure for the representative stress (3b), placing higher weight on the normal stress components. We argue that this approach has two major shortcomings.

First, the choice of the correct coordinate system is not trivial. As shown above for the hyperbolic contraction, the FS norm depends on the choice of the coordinate system, as shown above for the hyperbolic contraction. To define a consistent measure, the norm could, for instance, be applied in a local coordinate system aligned with the principal directions of the flow, as suggested

by Khoo et al. [11]. However, even this approach does not necessarily correspond to the actual extensional stress experienced by RBCs. This is because RBCs are not necessarily aligned with the flow direction. While it is true for the simple two-dimensional hyperbolic contraction from above, one could imagine superimposing the flow with a parallel flow out of the plane. This would change the mean flow velocity towards the out-of-plane direction. Nevertheless, the cell orientation and deformation would not change, as a parallel flow does not exert any deformation or rotation. Thus, the flow direction alone is not sufficient to determine the direction of normal and shear stress on RBCs. The more general approach in this sense is to employ a separate model to resolve RBC orientation, such as the TTM [7]. Here, the additional information of flow vorticity is taken into account to determine the orientation of RBCs based on an equilibrium between the moments of strain and vorticity.

Second, the coefficients of the weighting between shear stress and normal stress are based only on two special cases, i.e., simple shear ($\nu = 0$) and uniaxial extension ($\nu = 1$). They fail to capture the full range of possible flow conditions and in particular the vanishing effective stress in the presence of high vorticity $\nu \to -1$ (see Fig. 3b).

Instead, we are proposing a more universal approach based on flow vorticity. Our theory employs the observation that vorticity affects the orientation of RBCs in the flow. Thereby, the vorticity influences the portion of strain they experience and thus their deformation. In the plane Couette flow, the cells are at equilibrium between the opposing moments of strain and vorticity. As a result, they are not aligned with the principal direction of strain, so they do not experience the full tensile stress of the flow. Conversely, in the hyperbolic contraction, the cells align with the principal direction of strain, and they experience the full tensile stress of the flow, leading to overall higher deformation and ultimately higher hemolysis. This theory explains experimental observations [4, 6], and extends them to the full range of possible flow conditions. At the same time, it does not require any modifications to the norm for the scalar representative stress and does not depend on the choice of the coordinate system. It is applicable to any stress-based hemolysis model by correcting the representative stress (2) with the vorticity-dependent error:

$$\tau^* = (1 + \delta(\nu))\tau_{\mathrm{B}} \,,$$

with δ as given in Fig. 3b. We can thus incorporate results from more complex strain-based models into simple stress-based models. Nevertheless, strain-based models still retain advantages in modeling the viscoelastic deformation behavior of the cell membrane (see Fig. 1b), which is a feature of their differential equation structure (4a) and cannot be captured by algebraic stress-based models (2).

Evidently, the results presented here are highly idealized, specifically those in Fig. 3b. They represent steady state predictions of a strain-based cell morphology model that assumes ellipsoidal cell shape and no interaction between cells. While the results are qualitatively consistent with experimental observations and intuitively plausible, they need to be validated against more realistic models and experiments. More data is needed to determine the exact form of the vorticity-dependent error δ. This is subject of ongoing work.

Nevertheless, the results in Fig. 3b show a strong dependence of the effective stress on the vorticity. The analysis of the FDA pump in Fig. 4 shows large coherent regions which are consistently vorticity-dominated or strain-dominated. In these regions, stress-based models may overestimate or underestimate hemolysis, respectively. This suggests that vorticity needs to be taken into account when analyzing which regions are the most critical for hemolysis in ventricular assist devices (VADs).

5 Conclusion

We analyzed the effects of flow vorticity on hemolysis through a series of numerical experiments, comparing simple stress-based models to a more complex strain-based model. Flow vorticity affects RBC orientation and alignment, which in turn affects cell deformation through the direction of stresses that the cells experience. This causes uniaxial extensional flow to have a larger effect on RBC deformation than simple Coutte flow. We have developed a theory that systematically

quantifies the influence of vorticity on cell deformation and thus hemolysis. In short, it states that the effective stress experienced by RBCs monotonically decreases with the strength of the vorticity relative to the strain. This theory is consistent with experimental observations and extends them to the full range of possible flow conditions.

Overall, our results strongly suggest that vorticity significantly affects hemolysis, especially at higher stress levels. This is in contrast to well-established stress-based hemolysis models, which typically neglect the effects of varying vorticity. In this sense, this paper provides a foundation and a systematic framework for future research on the role of vorticity in hemolysis modeling.

Acknowledgment

This work was funded by Deutsche Forschungsgemeinschaft (DFG) through grant 333849990/GRK2379 (IRTG Hierarchical and Hybrid Approaches in Modern Inverse Problems).

References

[1] Bludszuweit, C.: Model for a General Mechanical Blood Damage Prediction. *Artificial Organs*, vol. 19, no. 7: (1995) pp. 583–589.

[2] Giersiepen, M., Wurzinger, L., Opitz, R. & Reul, H.: Estimation of Shear Stress-Related Blood Damage in Heart Valve Prostheses—In Vitro Comparison of 25 Aortic Valves. *International Journal of Artificial Organs*, vol. 13, no. 5: (1990) pp. 300–306.

[3] Ponnaluri, S. V., Hariharan, P., Herbertson, L. H., Manning, K. B., Malinauskas, R. A. & Craven, B. A.: Results of the Interlaboratory Computational Fluid Dynamics Study of the FDA Benchmark Blood Pump. *Annals of Biomedical Engineering*, vol. 51, no. 1: (2023) pp. 253–269.

[4] Lee, S. S., Yim, Y., Ahn, K. H. & Lee, S. J.: Extensional flow-based assessment of red blood cell deformability using hyperbolic converging microchannel. *Biomedical Microdevices*, vol. 11, no. 5: (2009) p. 1021.

[5] Down, L. A., Papavassiliou, D. V. & O'Rear, E. A.: Significance of Extensional Stresses to Red Blood Cell Lysis in a Shearing Flow. *Annals of Biomedical Engineering*, vol. 39, no. 6: (2011) pp. 1632–1642.

[6] Faghih, M. M. & Sharp, M. K.: Deformation of Human Red Blood Cells in Extensional Flow through a Hyperbolic Contraction. *Biomechanics and Modeling in Mechanobiology*, vol. 19, no. 1: (2020) pp. 251–261.

[7] Dirkes, N., Key, F. & Behr, M.: Eulerian formulation of the tensor-based morphology equations for strain-based blood damage modeling. *Computer Methods in Applied Mechanics and Engineering*, vol. 426: (2024) p. 116979.

[8] Arora, D., Behr, M. & Pasquali, M.: A Tensor-Based Measure for Estimating Blood Damage. *Artificial Organs*, vol. 28, no. 11: (2004) pp. 1002–1015.

[9] Taylor, G. I.: VIII. Stability of a viscous liquid contained between two rotating cylinders. *Philosophical Transactions of the Royal Society of London. Series A, Containing Papers of a Mathematical or Physical Character*, vol. 223, no. 605-615: (1997) pp. 289–343.

[10] Davey, A.: The growth of Taylor vortices in flow between rotating cylinders. *Journal of Fluid Mechanics*, vol. 14, no. 3: (1962) pp. 336–368.

[11] Khoo, D. P., Cookson, A. N., Gill, H. S. & Fraser, K. H.: Normal fluid stresses are prevalent in rotary ventricular assist devices: A computational fluid dynamics analysis. *The International Journal of Artificial Organs*, vol. 41, no. 11: (2018) pp. 738–751.